# Penetration of lightning MF signals to the upper ionosphere over VLF ground-based transmitters

Michel Parrot, U.S. Inan, N. G. Lehtinen, Jean-Louis Pinçon

# Penetration of lightning MF signals to the upper ionosphere over VLF ground-based transmitters

M. Parrot,[1,2] U. S. Inan,[3,4] N. G. Lehtinen,[3] and J. L. Pinçon[1,2]

[1]   The MF data recorded by the low-altitude satellite DEMETER have been used to survey the MF waves around the Earth. A global map of the MF emissions indicates that there exists a wave activity in the frequency range 2–2.5 MHz above the main powerful VLF ground-based transmitters operating in the frequency range 18–50 kHz. It is shown that this is due to the high-frequency part of whistlers induced by the thunderstorm activity. They can penetrate trough the ionosphere at the locations of the transmitters because these transmitters induce large ionospheric perturbations. This means that an integrated map over several months is able to show these MF emissions above all main VLF transmitters. The discrepancy between intensities of the emissions in winter and summer (in the Northern Hemisphere) is explained by considering the geographic variations of the plasma frequency below the satellite. It is shown that the MF waves spread in longitude in the hemisphere opposite to the VLF transmitters.

**Citation:**   Parrot, M., U. S. Inan, N. G. Lehtinen, and J. L. Pinçon (2009), Penetration of lightning MF signals to the upper ionosphere over VLF ground-based transmitters, *J. Geophys. Res.*, *114*, A12318, doi:10.1029/2009JA014598.

## 1.   Introduction

[2]   Thunderstorm activity is the most common phenomenon in the Earth's atmosphere. Resulting electromagnetic waves propagate in the Earth-ionosphere waveguide and also leak through the ionosphere into the overlying magnetosphere and can be observed in geomagnetically conjugate regions. Up to now, only few satellite observations exist of MF and LF emissions related to lightning. *Kotaki and Katoh* [1983] and *Kotaki* [1984] published the first maps of the MF emissions related to the lightning activity for the four seasons as well as maps of noise distributions. At ionospheric altitudes, *Kelley et al.* [1997] reported an MF observation of an EM pulse in connection with a lightning at a frequency less than 2 MHz.

[3]   It has been shown by *Fullekrug et al.* [2009] that LF waves coming from the Earth's surface (the LORAN pulses at 100 kHz) can be observed during nighttime in the upper ionosphere. In this article, we present maps of MF and LF electric fields recorded on the DEMETER satellite during nighttime, which show significant and persistent penetration of lightning MF signals, specifically over ground-based VLF transmitters. Results presented follow from and build upon previous observations of density irregularities in the vicinity of powerful VLF transmitters [*Parrot et al.*, 2007] and with MF data related to thunderstorm activity [*Parrot et al.*, 2008]. On one hand, *Parrot et al.* [2007] have shown that powerful ground-based VLF transmitters induce a dramatic perturbation of the plasma parameters in the nighttime ionosphere. On the other hand, MF pulses related to intense lightning strokes have been presented by *Parrot et al.* [2008]. They noted that these MF pulses (also just observed during nighttime) can reach the satellite altitude only if the strokes occur slightly equatorward from the satellite foot point, and only if the MF wave is not reflected below the satellite due to a high plasma frequency in the *F* layer.

[4]   The DEMETER payload is briefly described in section 2. Global maps are shown in section 3. Discussion and conclusions are provided in section 4.

## 2.   The Satellite DEMETER

[5]   DEMETER is a low-altitude satellite (710 km) launched in June 2004 onto a polar and circular orbit which measures electromagnetic waves and plasma parameters all around the globe, except in the auroral zones [*Parrot*, 2006]. Owing to technical reasons, data are only recorded at invariant latitudes less than 65°. The orbit of DEMETER is nearly sun-synchronous, and in this article, only the upgoing half-orbits corresponding to nighttime (2230 LT) are used. Concerning the electric field, the high-frequency (MF) detector range is from DC up to 3.33 MHz, whereas the VLF range is from 0 to 20 kHz. There are two scientific modes: a survey mode all around the globe and a burst mode when the satellite is above active seismic regions. The spectrum of one electric component is onboard computed in the MF and VLF ranges during the survey mode. During the burst mode, waveforms of the same electric field component are recorded up to 20 kHz in addition to the spectrum. The

[1]LPC2E, CNRS, Orléans, France.
[2]Also at University of Orleans, Orléans, France.
[3]Space, Telecommunications, and Radioscience Laboratory, Stanford University, Stanford, California, USA.
[4]Koç University, Istanbul, Turkey.
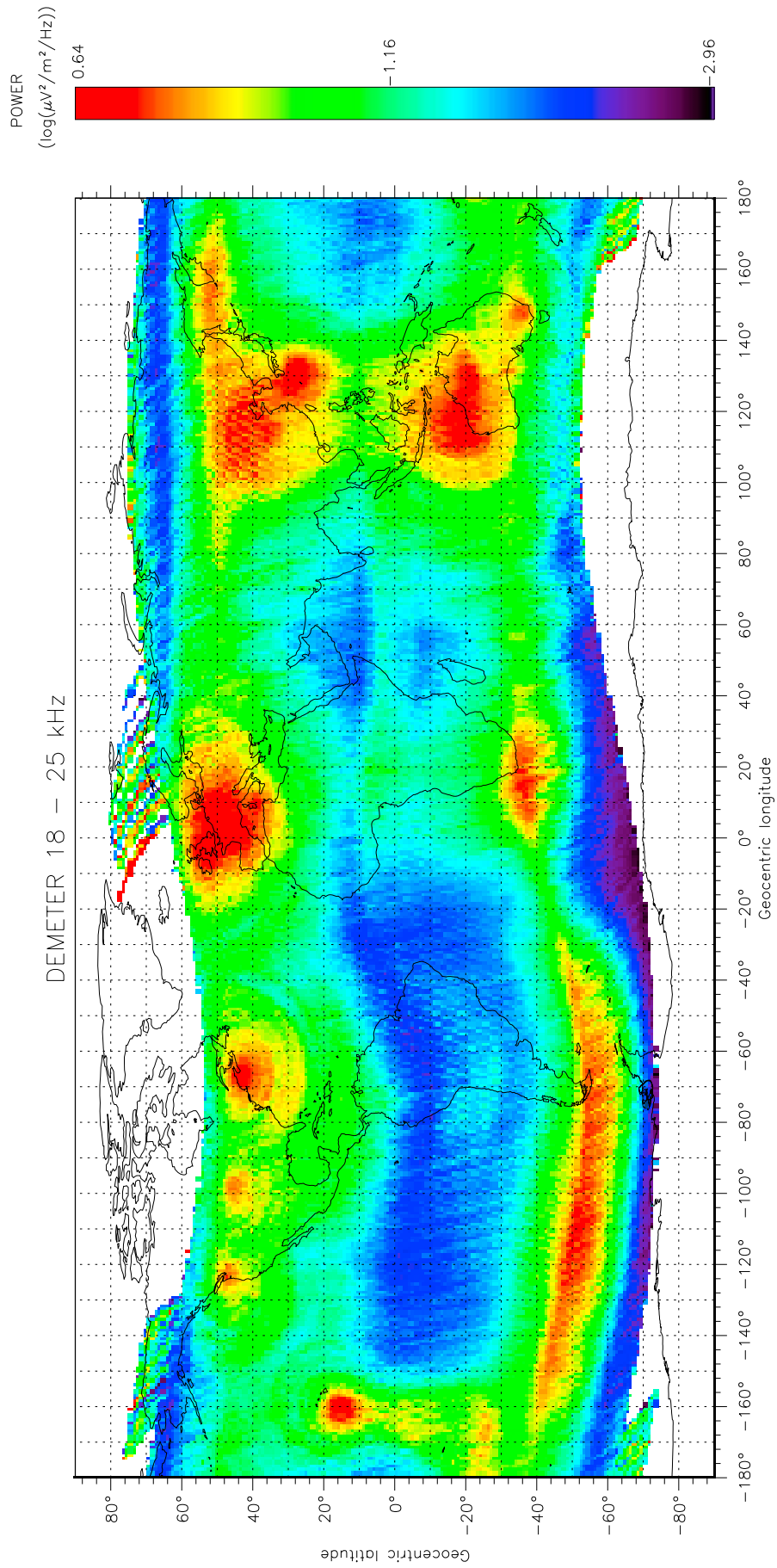
**Figure 1.** Global map of the emissions observed during nighttime and integrated in a frequency band between 18 and 25 kHz. The wave intensity is color coded according to the scale on the right.

**Table 1.** VLF Transmitters Seen in the Maps of Figures 1 and 2[a]

| Code | Name | Location | Frequency (kHz) | Power (kW) |
|------|------|----------|-----------------|------------|
| NPM | Lualualei | N21°25′ W158°09′ | 21.4 | 600 |
| NLK | Jim Creek | N48°12′ W121°55′ | 24.8 | 250 |
| NML | La Moure | N46°21′ W098°20′ | 25.2 | 500 |
| NAA | Cutler | N44°38′ W067°16′ | 24.0 | 1000 |
| NAU | Aquada | N18°23′ W067°10′ | 40.75 | 100 |
| GQD | Anthorn | N54°54′ W003°16′ | 19.6 | 500 |
| HWU | Rosnay | N46°42′ E001°14′ | 18.3 | 400 |
| DHO | Rhauderfehn | N53°04′ E007°36′ | 23.4 | 500 |
| NSY | Niscemi | N37°07′ E014°26′ | 45.9 | |
| NWC | North West Cape | S21°48′ E114°09′ | 19.8 | 1000 |
| NDT | Ebino | N32°04′ E130°49′ | 22.2 | |
| NTS | Woodside | S38°28′ E146°56′ | 18.6 | |
| UBE | Petropavlovsk | N52°55′ E158°39′ | 16.2 | |

[a]Transmitters are listed from the left to the right according to their locations on the maps. When it is noted, the power is only indicative as most of these transmitters are used by the army (navy) of different countries.

burst mode allows performing a spectral analysis with higher time and frequency resolution. In MF, the signals are sampled at 6.66 MHz and digitized with 8 bits. The MF data acquisition is performed on 40-data snapshots, each 0.6144 ms long and evenly spaced in the 2.048 s elementary interval of the VLF channel acquisition. Individual power spectra are calculated for each snapshot with a frequency resolution of 3.25 kHz and averaged to provide a power spectrum every 2.048 s. In burst modes, the averaged power spectrum and waveform data for a single 0.6144 ms interval are available. In survey modes, the power spectra are the only information available. Whatever the mode, a neural network gives the times of the 0+ whistlers and one-hop whistlers recorded on the satellite with their associated dispersions, with a temporal accuracy of the order of 0.1 s [*Elie et al.*, 1999]. This neural network uses as input the individual VLF spectra of the selected electric component, which are onboard computed and then averaged to produce the final spectrum sent in the telemetry. Details of the wave experiment can be found in the work of *Parrot et al.* [2006] and *Berthelier et al.* [2006].

## 3. The Global Maps

[6] Figure 1 shows the global map of the wave intensity measured by an electric component during nighttime between 18 and 25 kHz. The resolution of the map is 1° in latitude and 1° in longitude. The data cover the 3 years 2006, 2007, and 2008, which were very quiet in terms of geomagnetic activity. In the region of the Americas, the peaks in intensity in the Northern Hemisphere correspond to the locations of powerful VLF transmitters (see Table 1). The prominent VLF signal levels in the Southern Hemisphere conjugate regions are the corresponding signals that have propagated along approximately field-aligned raypaths, with substantial spreading in longitude but confinement to a relatively small band of *L*-shells. In Europe, the powerful transmitters are relatively close to one another (Table 1) so that a single broad peak is observed. The corresponding Southern Hemisphere conjugate region of the European peak is also evident. Farther to the east, Australia is the only country in the Southern Hemisphere where there are

two VLF transmitters, which both produce VLF peaks, together with the corresponding geomagnetically conjugate regions. For transmitters located at the lowest latitudes, such as NPM in Hawaii, the approximately field-aligned magnetospheric propagation paths can often cross the satellite altitude, as manifested in the form of streaks of VLF energy connecting the high-field regions in the parent and conjugate hemispheres. Apart from the known VLF transmitters, we note localized peaks in VLF energy at high invariant latitudes (>65°) in Alaska and Norway, corresponding to special campaigns for VLF generation experiments conducted by the HF heating facilities at the High frequency Active Auroral Research Program and European Incoherent Scatter [see, e.g., *Piddyachiy et al.*, 2008].

[7] Figure 2 presents the same map as in Figure 1, but for the frequency range 2000–2500 kHz. Surprisingly, this map of 2–2.5 MHz wave energy also shows wave-localized enhancements at the locations of the VLF transmitters and their conjugate regions. It should be noted that these enhancements are only ∼3 dB above the average background, but nevertheless, they are clearly evident. In addition to the VLF transmitters observed in Figure 1, two others become visible (NAU and NSY), which cannot be seen in Figure 1 because they operate at frequencies larger than the 40 kHz upper limit used for Figure 1 (see Table 1). Since the VLF transmitters do not produce any radiation in the 2–2.5 MHZ range, the enhanced wave energy observed on DEMETER must be due to signals from other sources, the transionospheric propagation of which has been somehow facilitated by the presence of the enhanced VLF radiation in these regions. One possible source of such MF energy is lightning discharges, and observation of MF impulses of lightning origin on DEMETER has recently been reported [*Parrot et al.*, 2008]. DEMETER observations have also revealed the formation of electron density irregularities over powerful VLF transmitters [*Parrot et al.*, 2007], and it is possible that MF impulses of lightning origin may be funneled upward via these irregularities.

[8] In order to assess the possibility of lightning origin for the MF waves observed, the data displayed in Figure 2 were sorted for different seasons. Figure 3 (top) shows the data in the same frequency range, but for summer in the Northern Hemisphere (average values of the months 6, 7, 8, and 9 of the years 2006, 2007, and 2008), while Figure 3 (bottom) shows data for winter in the North Hemisphere (months 1, 2, 11, and 12 of the years 2006, 2007, and 2008). Owing to a known problem of MF interference induced by the solar panel when it is lit up, the data have been suppressed at high latitudes in the north during summertime and in the south during wintertime. Remarkably enough, the result in Figure 3 appears at first thought not to be consistent with the hypothesis of lightning origin for the MF enhancements; the localized MF energy peaks around the North American VLF transmitters are, in fact, more prominent during wintertime, when the lightning activity is at its lowest [*Christian et al.*, 2003].

[9] On the other hand, close examination of data from individual passes clearly suggests that the observed MF energy enhancements are, in fact, MF impulses of lightning origin. As mentioned earlier, *Parrot et al.* [2007] have shown that VLF ground-based transmitters produce density irregularities in their overhead ionospheres, which extend at
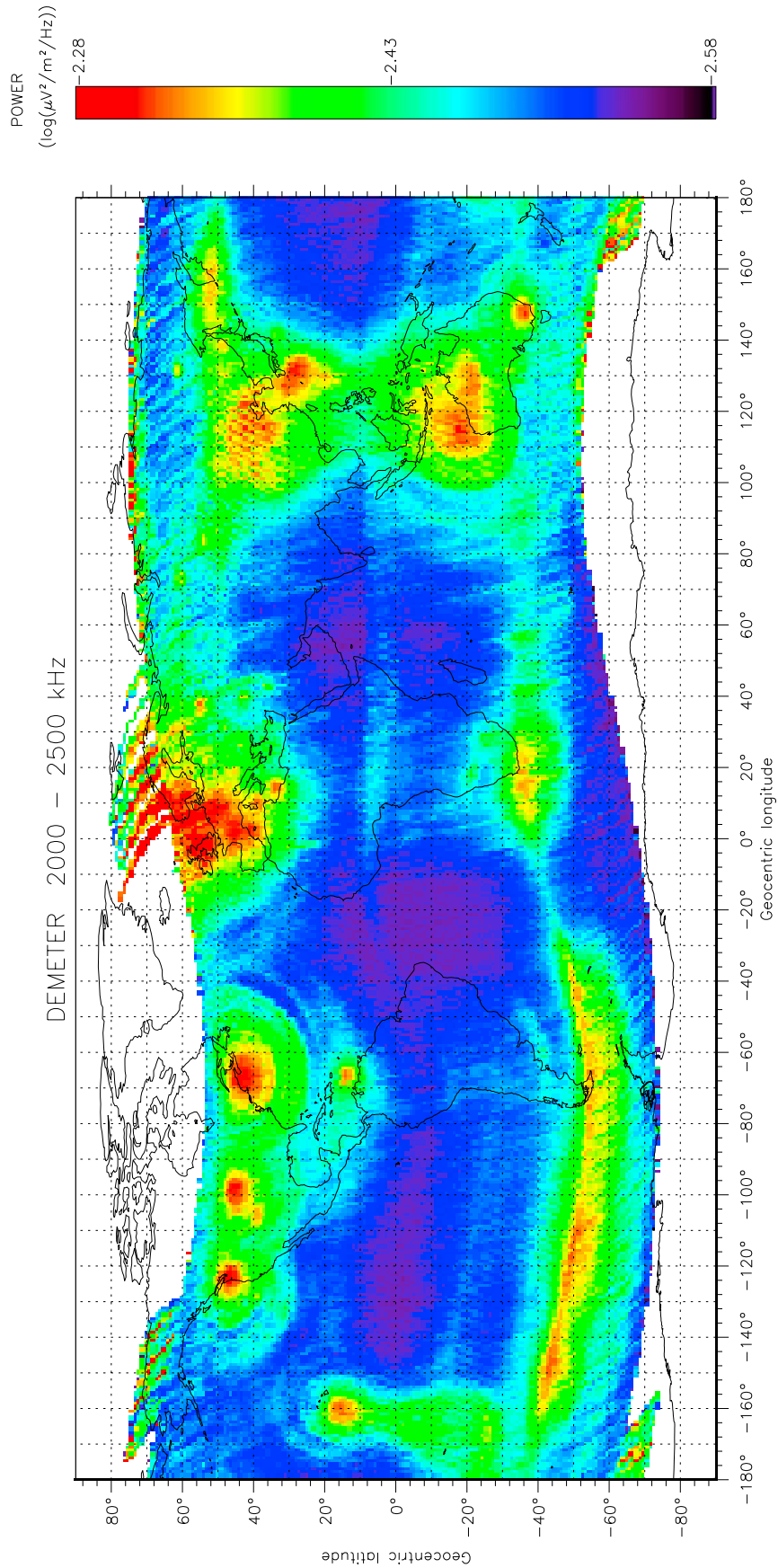
**Figure 2.** Global map of the emissions observed during nighttime and integrated in a frequency band between 2 and 2.5 MHz. The wave intensity is color coded according to the scale on the right.
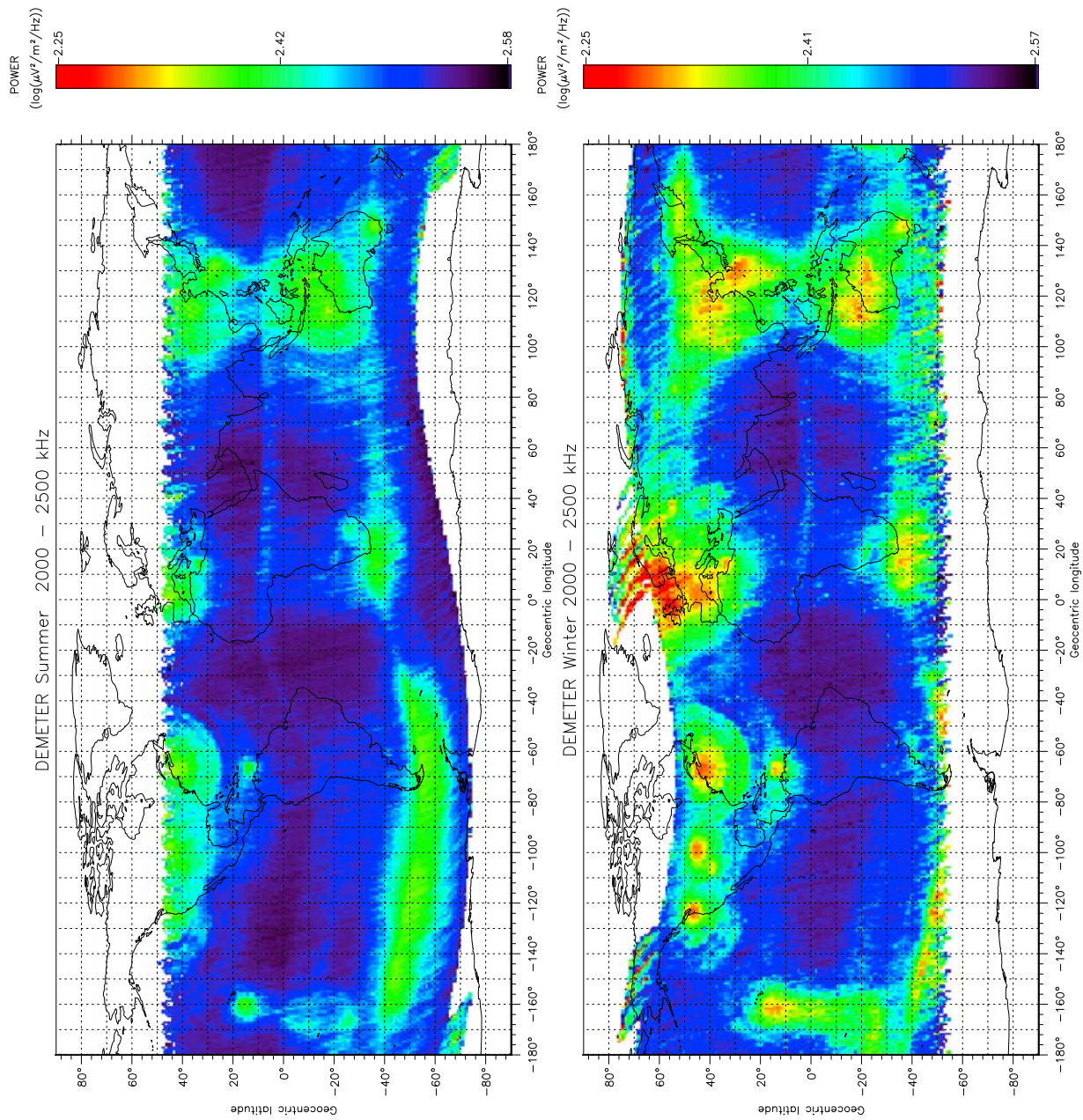
**Figure 3.** (top) Global map of the emissions observed during nighttime and integrated in a frequency band between 2 and 2.5 MHz when it is summer in the Northern Hemisphere. The wave intensity is color coded according to the scale on the right. (bottom) Same as Figure 3 (top), but when it is winter in the Northern Hemisphere.
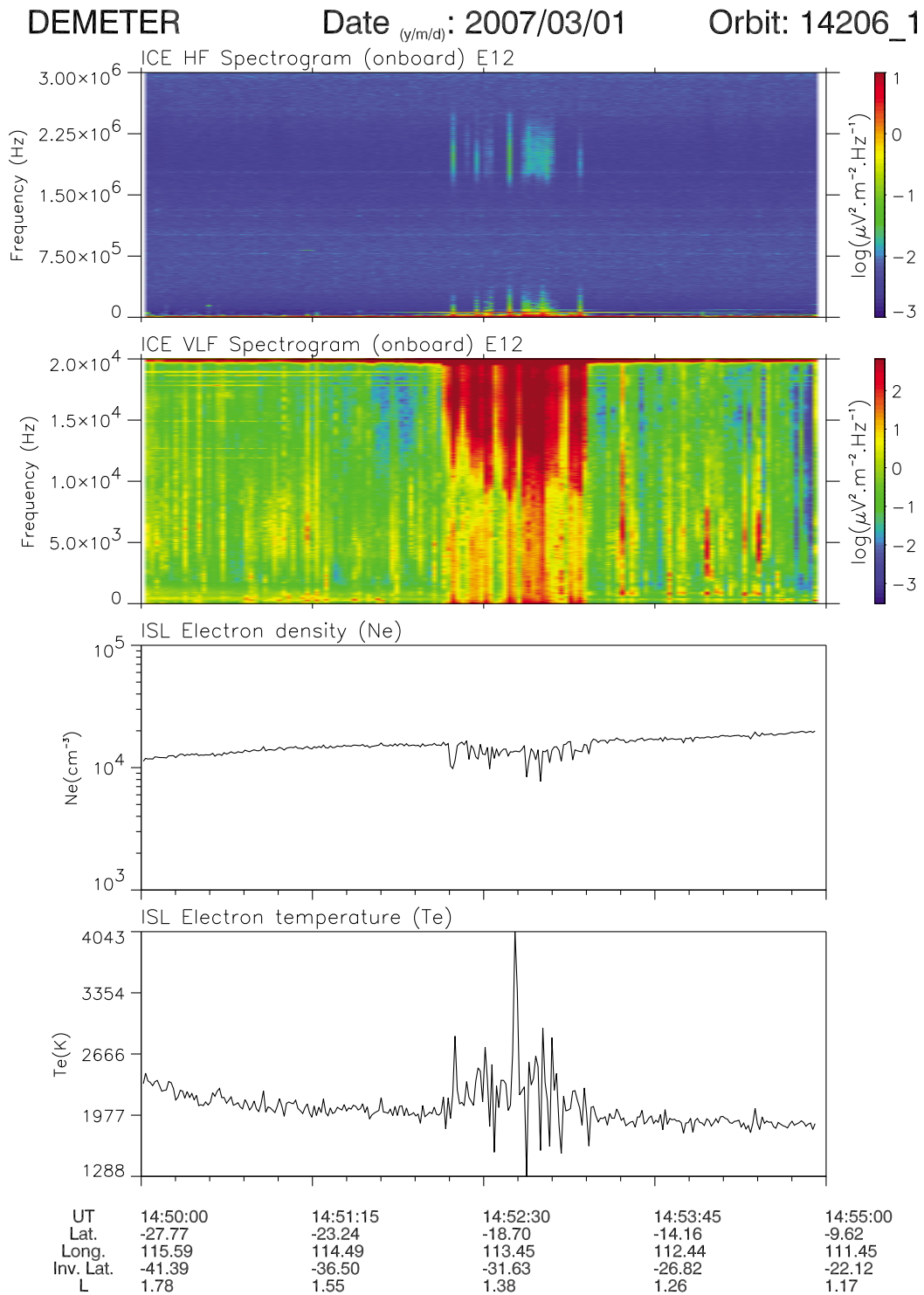
**Figure 4.** Data recorded on 1 March 2007 between 1450 and 1455 UT. Shown are the MF spectrogram of one electric component up to 3 MHz (first panel), the VLF spectrogram of the same component up to 20 kHz (second panel), the electron density (third panel), and the electron temperature as a function of time (fourth panel). The parameters below the spectrogram (UT, geographical latitude and longitude, invariant latitude and the McIlwain parameter, *L*) indicate that the observation takes place during nighttime north of the NWC location (see Table 1).
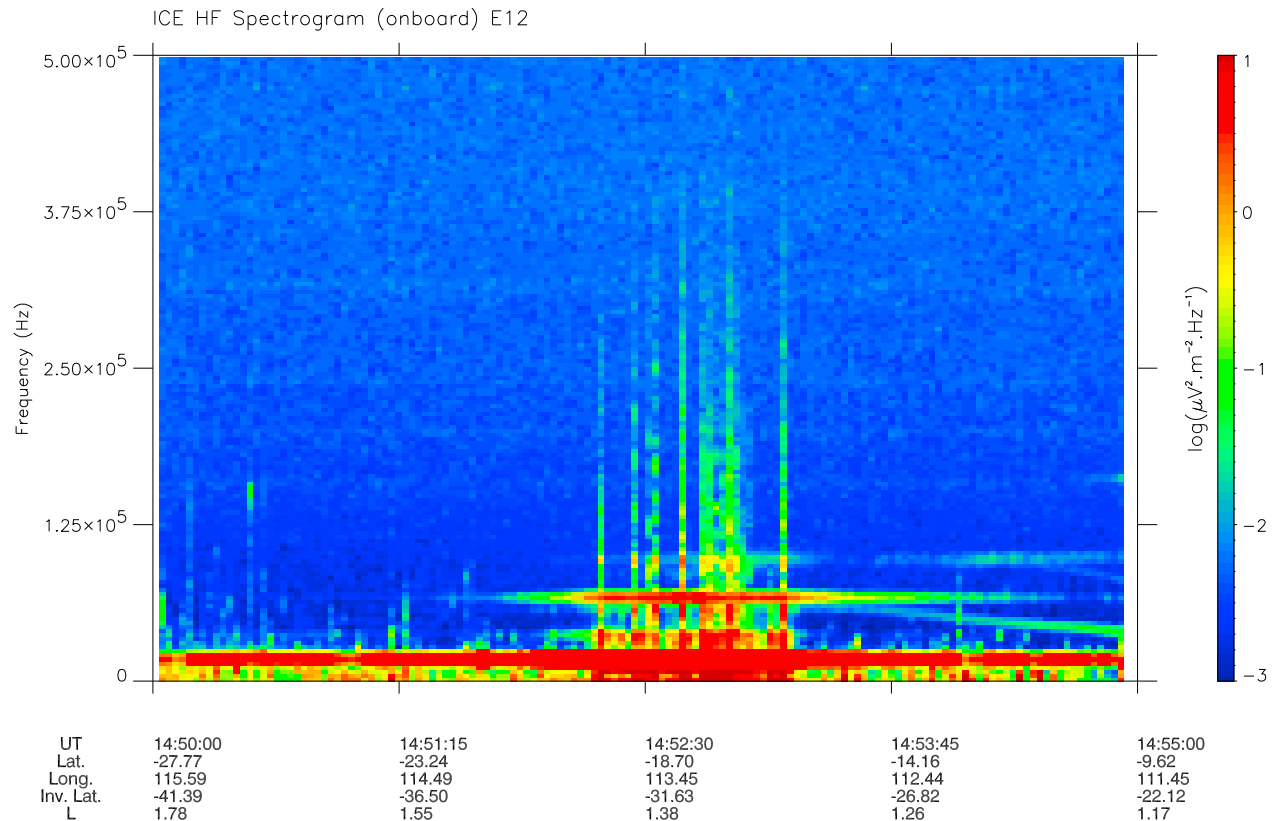
**Figure 5.** Frequency zoom concerning the lower-frequency part of Figure 4a.

least up to 700 km during nighttime. Figure 4 presents another example of these ionospheric perturbations recorded close to the VLF transmitter NWC on 1 March 2007 between 1450 and 1455 UT. Figure 4 (first panel) shows a MF spectrogram showing data from an electric component. Figure 4 (second panel) is a VLF spectrogram mainly dominated by sferics and whistlers (vertical lines). On the top, one can see the frequency of the transmitter (horizontal line at 19.8 kHz). Figure 4 (third panel) concerns the electron density given by a Langmuir probe [*Lebreton et al.*, 2006], whereas Figure 4 (fourth panel) is related to the electron temperature. It is evident from Figure 4 that the VLF transmitter induces a heating of the ionosphere and that close to the transmitter, the intensities of the LF and MF sferics are enhanced. Figure 5 shows in more detail the lower part of the MF range, and at the location of the perturbation, one can also observe that a signal at a frequency ~66 kHz (coming from a transmitter located in China) is also apparent more intensely in the same region overhead the VLF transmitter. This observation indicates that the transionospheric escape of all waves propagating in the Earth-ionosphere waveguide is enhanced near the location of the density perturbations produced by the VLF transmitters. It must be noticed that this location is different from the location of particle precipitation induced by this transmitter [*Inan et al.*, 1984; *Kulkarni et al.*, 2008; *Sauvaud et al.*, 2008].

[10] Besides the LF and MF ranges of frequencies, there is also a broadband enhancement in the VLF range in the vicinity of transmitters (Figure 4, second panel). This enhancement may have two different interpretations: (1) First, we may assume that these are lightning sferics, and an enhancement is therefore due to a lower attenuation of VLF waves. The regions of lower attenuation coincide with the locations of density and temperature irregularities. Most of the attenuation of VLF waves occurs in the ionospheric $D$ and $E$ regions and is due to electron-neutral collisions. This hypothesis then leads us to conclude that the observed electron density depletions extend from the $F$ region all the way down to the $D$ and $E$ regions. (2) The second interpretation of VLF enhancements is that they represent Doppler-shifted narrow-band electric fields. The wave-normal vectors of these waves have to be of large enough magnitude and have random direction in order to obtain high Doppler shifts, $\Delta f = -(\mathbf{k}.\mathbf{v})/2\pi$, where $\mathbf{v}$ is the velocity of the satellite. These could be either electrostatic fields that are present in the irregularities, similar to those observed by *Pfaff et al.* [2008], or quasi-electrostatic whistler mode (QEWM) waves, which have been produced by the scattering of VLF transmitter waves from the ionospheric irregularities [e.g., *Bell and Ngo*, 1990]. Neither of these waves has significant magnetic field components (see the appendix).

[11] Furthermore, the MF spectrogram (Figure 4, first panel) indicates that at the time of these whistler mode
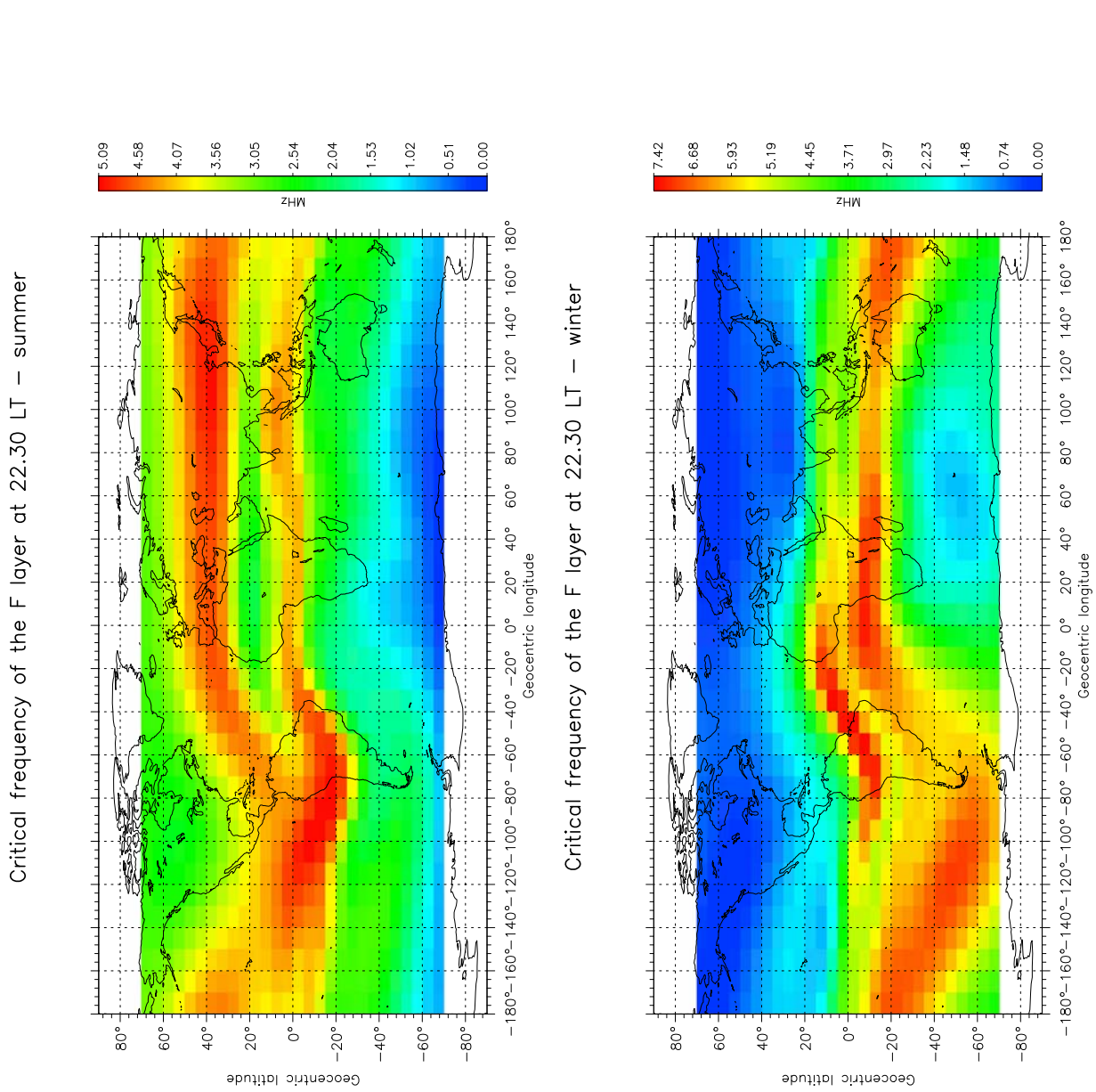
**Figure 6.** Global maps of the critical frequency of the *F* layer at 2230 LT given by the IRI model. (top) Summertime (August) in the Northern Hemisphere. (bottom) Wintertime (December) in the Northern Hemisphere.
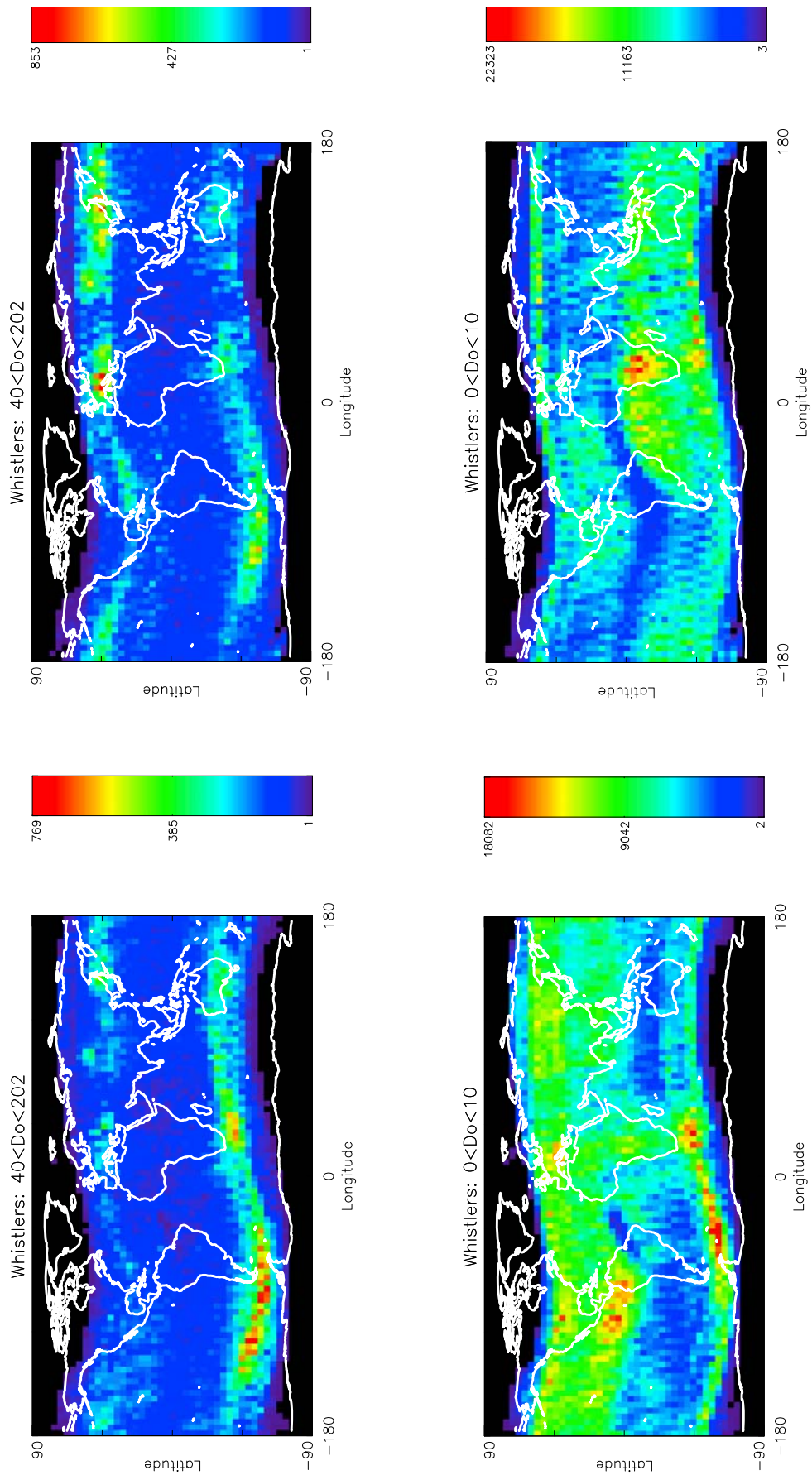
**Figure 7.** Global maps of the number of whistlers recorded by the neural network onboard DEMETER. (left) Summer 2008 in the Northern Hemisphere and (right) winter 2008 in the Northern Hemisphere. (top) Whistlers with high dispersion (40 < Do < 202) and (bottom) whistlers with low dispersion (0 < Do < 10). The color scales at the right give the number of whistlers. Low-dispersion whistlers (Figure 7, bottom) mean that these whistlers are just coming from below. On the left side (summertime), as there is no significant thunderstorm activity in the conjugate part of the United States (Figure 7, bottom), high whistler dispersion observed in this region (Figure 7, top) means that these whistlers are coming from the opposite hemisphere.

signals, there are MF pulses starting at around 1.8 MHz. These MF pulses are the high-frequency part of the electromagnetic pulses generated at the time of the lightning strokes, i.e., they may be the frequency continuation of the whistlers observed in the VLF range, if the first interpretation of the VLF enhancements outlined previously is correct. A superposition of these MF pulses is what constitutes the wave energy enhancements that are observed in the global map of the Earth at the locations of the main VLF ground-based transmitters when DEMETER MF data are averaged over months.

[12] In Figure 3, a slight difference is observed between summer and winter in the Northern Hemisphere. The MF intensity is lower during summertime if one checks, for example, above the United States and Europe. This result is at first counterintuitive and unexpected since thunderstorm activity is more intense during summertime. The reason for this opposite variation may possibly lie in the upward propagation of the MF waves, which would be determined by the maximum plasma frequency in the $F$ region of the ionosphere. Maps of the plasma frequency of the $F$ layer below the satellite are plotted in Figure 6 using the IRI model [*Bilitza*, 2001]. Figure 6 (top) is related to summertime, whereas Figure 6 (bottom) is for wintertime in the Northern Hemisphere. Both Figures 6 (top) and 6 (bottom) correspond to the local time of the satellite at nighttime. It can be seen that during summer, the plasma frequency (i.e., electron density) is relatively high and thus can prevent the MF waves from reaching the altitude of the satellite. On the contrary, during winter, the plasma frequency above the United States and Europe is low, thus allowing the propagation of MF waves to satellite altitude, as exhibited with prominent peaks around VLF transmitters during wintertime, even if the number of lightning strokes is lower than during summer.

[13] It can be also seen in Figure 6 (bottom) that the plasma frequency is very high in the region conjugate to the continental United States and that this prevents MF waves (originating in lightning activity during summertime in the Southern Hemisphere) from reaching the satellite. MF waves at a frequency larger than the plasma frequency are reflected. The MF waves observed in the region conjugate to the continental United States are thus due to propagation from the Northern Hemisphere even during winter. This result can also be seen in Figure 7, which gives the number of whistlers recorded by DEMETER within a given dispersion range, as analyzed by the onboard neural network system [*Elie et al.*, 1999]. In Figure 7 (bottom left), showing summer in the Northern Hemisphere, a large number of whistlers with small dispersion (essentially upgoing 0+ whistlers [*Smith and Angerami*, 1968]) are observed above the United States and below in the tropical region. The corresponding whistlers with high dispersion can be seen in Figure 7 (top left). These highly dispersed whistlers are observed at high latitudes in the region conjugate to the continental United States. It should be noted, however, that even during wintertime (Figure 7, right), there is a nonnegligible thunderstorm activity over the continental United States, which accounts for highly dispersed whistlers seen in the Southern Hemisphere, as displayed in Figure 7 (top right). These whistlers are clearly not from lightning in the Southern Hemisphere since Figure 7 (bottom right) does not

indicate detection of whistlers with low dispersion in this region.

## 4.   Discussion and Conclusions

[14] We have proposed that the observations of enhanced MF radiation in regions conjugate to the VLF transmitters in the American sector in Figure 2 may be due to transionospheric propagation facilitated by density irregularities produced by the effect of waves from VLF transmitters. This proposed mechanism supposes that the MF waves propagated through the magnetosphere from the Northern Hemisphere along field-aligned ducts. The electron density in the magnetosphere is small, and therefore the plasma frequency is small compared to the MF frequency (for $f = 2.5$ MHz and $N_e = 10^9$ m$^{-3}$, we have $X = f_p^2/f^2 \approx 0.013$). Thus the refractive index of MF waves $n \approx (1 - X)^{1/2}$ is close to 1 (neglecting the effect of the geomagnetic field), and density gradients perpendicular to the geomagnetic field are required for the MF wave to remain ducted along the field lines. For a curvature radius of the field line $R$, we can obtain a condition on the rate of change of the refractive index in the direction perpendicular to field lines. For waves parallel to the geomagnetic field, we have $dn/dR < -n/R$, from which $dN_e/dR > 2N_e/XR \approx 150 N_e/R$ [*Voge*, 1961], which is not a very strict condition since the characteristic perpendicular size of the irregularity, $D = N_e(dN_e/dR)^{-1}$, is not required to be too large, $D < R/150$, which, for $R \sim R_{\text{Earth}}$, becomes $D < 40$ km (or 4 km for a 10% change in $N_e$). Another condition is the absence of small-scale irregularities inside the duct on which the MF wave may scatter and leave the duct. This is because for MF waves to be guided, the wave-normal vector has to be almost parallel to the geomagnetic field, and the scattering on longitudinal irregularities may change the direction of the wave-normal vector.

[15] A global map of the Earth at MF frequencies has been obtained with data recorded by the low-altitude satellite DEMETER during nighttime. Even if the frequency range of this map (2–2.5 MHz) is far from the frequency range of the VLF ground-based transmitters (18–50 kHz), this map indicates that the MF wave intensity is slightly enhanced at the position of the most powerful ones. Our analyses indicate that the observed MF enhancements are likely due to the ionospheric perturbations generated by the ground-based VLF transmitters. The intense VLF radiation from the transmitters creates irregularities which act as chimneys in the ionosphere through which the MF part of the whistler waves induced by the thunderstorm activity can escape and reach the satellite at 700 km altitude. These MF waves from thunderstorm activity are ducted along field-aligned irregularities and are observed in the conjugate regions. The leakage in and out of a multitude of such ducts accounts for the observed spread in longitude.
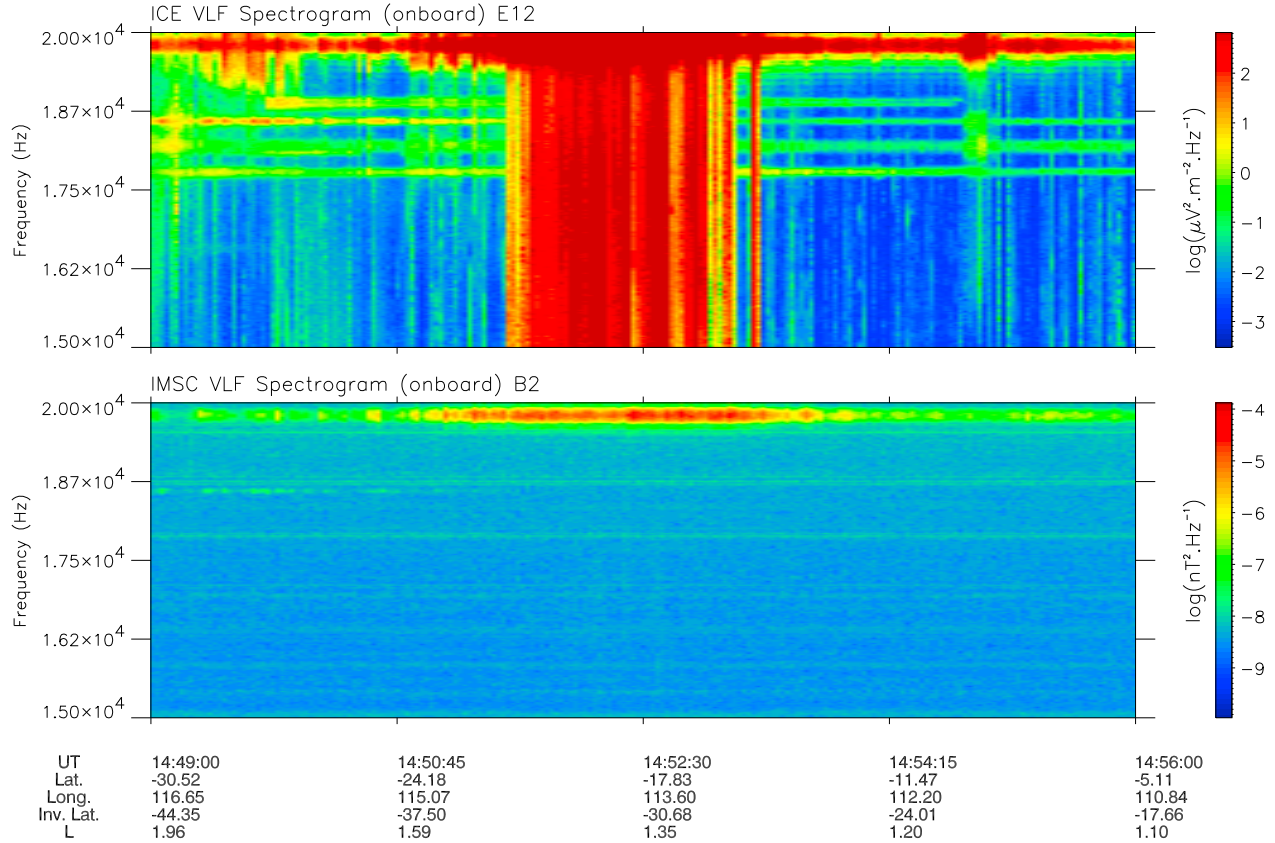
## Appendix A:   Observation of Quasi-electrostatic Whistler Mode Waves

[16] Figure A1 shows the upper part of the electric and magnetic VLF spectrograms recorded in the vicinity of NWC (frequency of emission $f_0 = 19.8$ kHz). This plot indicates that there is no broadband magnetic signal; only

**DEMETER**                              **Date** (y/m/d)**: 2006/09/22**                              **Orbit: 11856_1**



**Figure A1.** (top) Electric and (bottom) magnetic spectrograms recorded on 22 September 2006 between 1449 and 1456 UT and in a frequency range between 15 and 20 kHz. The parameters below the spectrograms are UT, the geographical latitude and longitude, the invariant latitude, and the McIlwain parameter, $L$. This event is described in detail in the work of *Parrot et al.* [2007].

a narrowband signal is seen at the VLF transmitter frequency. This is consistent with QEWM waves, as explained subsequently.

[17] If $\mathbf{n} = \mathbf{k}c/\omega$ is the refractive index vector, then to get the observed Doppler shift, $\Delta f/f_0 = (\mathbf{n}.\mathbf{v})/c \sim 1$ (where $\mathbf{v}$ is the DEMETER velocity), we need $n = |\mathbf{n}| \sim 3 \times 10^4$. It is much higher than the 0+ whistler refractive index $n_w \sim 30$, and this indicates that these waves are close to the resonance cone; that is, they are QEWM waves.

[18] For QEWM waves, an estimation from the Appleton-Hartree equation (under the valid, in our case, assumptions $f_0 \ll f_H \ll f_p$, where $f_H$ and $f_p$ are the electron gyro and plasma frequencies, respectively) gives $cB/E \approx 2^{1/2} n_w^2/n$; that is, the magnetic field is proportional to $f_0/\Delta f$. The further we are away from VLF transmitter frequency $f_0$, the dimmer is the magnetic field. Assuming that $E$ has a uniform spectral power density (as seen in Figure A1, top), the spectral power density of $B$ should fall off as $\Delta f^{-2}$.

[19] A numerical estimation using the experimental values of Figure A1 is now done. For the electric field power density $P(E) = 10^3 \ \mu V^2/m^2/Hz$, and using $n_w = 30$, far from from $f_0$, we must have $P(B) = 2(n_w^2/n/c)^2 \ P(E) \sim 2 \times 10^{-11} \ nT^2/Hz$, which is well below the noise level in Figure A1 (bottom). Whereas at $f_0$, for 0+ whistler waves, we have $cB/E = n_w$, and we must have $P(B) = (n_w/c)^2 *$

$P(E) \sim 10^{-5} \ nT^2/Hz$, which is consistent with the value in Figure A1 (bottom).

## References

Bell, T. F., and H. D. Ngo (1990), Electrostatic lower hybrid waves excited by electromagnetic whistler mode waves scattering from planar magnetic-field-aligned plasma density irregularities, *J. Geophys. Res.*, *95*, 149–172, doi:10.1029/JA095iA01p00149.

Berthelier, J. J., et al. (2006), ICE, The electric field experiment on DEMETER, *Planet. Space Sci.*, *54*, 456–471, doi:10.1016/j.pss.2005.10.016.

Bilitza, D. (2001), International Reference Ionosphere 2000, *Radio Sci.*, *36*, 261–275, doi:10.1029/2000RS002432.

Christian, H. J., et al. (2003), Global frequency and distribution of lightning as observed from space by the Optical Transient Detector, *J. Geophys. Res.*, *108*(D1), 4005, doi:10.1029/2002JD002347.

Elie, F., M. Hayakawa, M. Parrot, J. L. Pinçon, and F. Lefeuvre (1999), Neural network system for the analysis of transient phenomena onboard the DEMETER micro-satellite, *J. IEICE E*, *82-A*, 1575–1581.

Fullekrug, M., M. Parrot, M. Ash, I. Astin, P. Williams, and R. Talhi (2009), Transionospheric attenuation of 100 kHz radio waves inferred from satellite and ground based observations, *Geophys. Res. Lett.*, *36*, L06104, doi:10.1029/2008GL036988.

Inan, U. S., H. C. Chang, and R. A. Helliwell (1984), Electron precipitation zones around major ground-based VLF signal sources, *J. Geophys. Res.*, *89*, 2891–2906, doi:10.1029/JA089iA05p02891.

Kelley, M. C., S. D. Baker, R. H. Holzworth, P. Argo, and S. A. Cummer (1997), LF and MF observations of the lightning electromagnetic pulse at ionospheric altitudes, *Geophys. Res. Lett.*, *24*, 1111–1114, doi:10.1029/97GL00991.

Kotaki, M. (1984), Global distribution of atmospheric radio noise derived from thunderstorm activity, *J. Atmos. Terr. Phys.*, *46*, 867–877, doi:10.1016/0021-9169(84)90026-6.

Kotaki, M., and C. Katoh (1983), The global distribution of thunderstorm activity observed by the ionosphere sounding satellite (ISS-b), *J. Atmos. Terr. Phys.*, *45*, 833–847.

Kulkarni, P., U. S. Inan, T. F. Bell, and J. Bortnik (2008), Precipitation signatures of ground-based VLF transmitters, *J. Geophys. Res.*, *113*, A07214, doi:10.1029/2007JA012569.

Lebreton, J. P., et al. (2006), The ISL Langmuir probe experiment and its data processing onboard DEMETER: Scientific objectives, description and first results, *Planet. Space Sci.*, *54*, 472–486, doi:10.1016/j.pss.2005.10.017.

Parrot, M. (Ed.) (2006), First results of the DEMETER micro-satellite, *Planet. Space Sci.*, 54(5).

Parrot, M., et al. (2006), The magnetic field experiment IMSC and its data processing onboard DEMETER: Scientific objectives, description and first results, *Planet. Space Sci.*, *54*, 441–455, doi:10.1016/j.pss.2005.10.015.

Parrot, M., J. A. Sauvaud, J. J. Berthelier, and J. P. Lebreton (2007), First in-situ observations of strong ionospheric perturbations generated by a powerful VLF ground-based transmitter, *Geophys. Res. Lett.*, *34*, L11111, doi:10.1029/2007GL029368.

Parrot, M., U. Inan, N. Lehtinen, E. Blanc, and J. L. Pinçon (2008), MF signatures of powerful lightning recorded on DEMETER, *J. Geophys. Res.*, *113*, A11321, doi:10.1029/2008JA013323.

Pfaff, R., C. Liebrecht, J.-J. Berthelier, M. Malingre, M. Parrot, and J.-P. Lebreton (2008), DEMETER satellite observations of plasma irregularities in the topside ionosphere at low, middle, and sub-auroral latitudes and their dependence on magnetic storms, in *Midlatitude Ionospheric Dynamics and Disturbances*, *Geophys. Monogr. Ser.*, vol. 181, edited by P. M. Kintner et al., pp. 297–310, AGU, Washington, D. C.

Piddyachiy, D., U. S. Inan, T. F. Bell, N. G. Lehtinen, and M. Parrot (2008), DEMETER observations of an intense upgoing column of ELF/VLF radiation excited by the HAARP MF heater, *J. Geophys. Res.*, *113*, A10308, doi:10.1029/2008JA013208.

Sauvaud, J.-A., R. Maggiolo, C. Jacquey, M. Parrot, J.-J. Berthelier, R. J. Gamble, and C. J. Rodger (2008), Radiation belt electron precipitation due to VLF transmitters: Satellite observations, *Geophys. Res. Lett.*, *35*, L09101, doi:10.1029/2008GL033194.

Smith, R. L., and J. J. Angerami (1968), Magnetospheric properties deduced from OGO 1 observations of ducted and nonducted whistlers, *J. Geophys. Res.*, *73*, 1–20, doi:10.1029/JA073i001p00001.

Voge, J. (1961), Propagation guidée le long d'un feuillet atmosphérique ou (plus particulièrement) exosphérique: Première partie, *Ann. Telecommun.*, *16*, 288–295, doi:10.1007/BF03010026.

———————————

U. S. Inan and N. G. Lehtinen, Space, Telecommunications, and Radioscience Laboratory, Packard Building, Room 355, 350 Serra Mall, Stanford University, Stanford, CA 94305-9515, USA.

M. Parrot and J. L. Pinçon, LPC2E/CNRS, 3A Avenue de la Recherche, F-45071 Orléans CEDEX 2, France. (mparrot@cnrs-orleans.fr)